Dynamic modelling and validation of pre-combustion CO_2 absorption based on a pilot plant at the Buggenum IGCC power station

Carsten Trapp [a,*], Carlo de Servi [a], Francesco Casella [b], André Bardow [c], Piero Colonna [a,*]

[a] *Delft University of Technology, Propulsion and Power, 2629 HS Delft, The Netherlands*
[b] *Politecnico di Milano, Dipartimento di Elettronica, Informazione e Bioingegneria, 20133 Milano, Italy*
[c] *RWTH Aachen University, Institute of Technical Thermodynamics, 52056 Aachen, Germany*

Received 28 May 2014 Received in revised form 14 November 2014
Accepted 10 February 2015

1. Introduction

In order to mitigate the effects of climate change attributed to the anthropogenic combustion of fossil fuels carbon capture and storage (CCS) is identified as one of the potential technolo-gies (International Energy Agency, 2012). CCS is considered as transitional technology until the energy demand is fully supplied by renewable sources. Some of the technologies required for CO_2 capture are already applied commercially in the chemical industry, such as CO_2 absorption, and can be considered well proven. Moreover, recently CO_2 capture from power plants has been utilized in combination with enhanced oil recovery (Whittakera et al., 2011). In the face of commercial-scale application in the power sector, various aspects are currently studied, such as pro-cess energy efficiency, plant complexity and operational flexibility. For the successful implementation of CCS also challenges related to economic viability, public acceptability, uncertainties in policies and regulations need to be overcome.

Among the CO_2 capture technologies, pre-combustion CO_2 capture applied to integrated gasification combined cycle (IGCC) power plants is a promising technical solution due to its potential for high net efficiency (Damen et al., 2006; NETL, 2013). Moreover, IGCC power plants feature advantages regarding fuel flexibility and low emission of other air pollutants in comparison to conventional pulverized coal steam power plants. The integration of the capture unit into the very complex gasification process and combined cycle power plant leads to challenging problems as far as

* Corresponding authors. Tel.: +31 152782172.
E-mail addresses: C.Trapp@tudelft.nl (C. Trapp), P.Colonna@tudelft.nl (P. Colonna).

Nomenclature

Δp	pressure drop, Pa
a	specific surface area, $m^2\ m^{-3}$
C	constant
d	diameter, m
F_V	gas/vapour capacity factor, $Pa^{-0.5}$
Fr	Froude number
g	gravitational acceleration, $m\ s^{-2}$
H	height, m
ho_L	column holdup, $m^3\ m^{-3}$
K	wall factor
M	total mass, kg
m	mass flow rate, kg/s
p	pressure, Pa
Re	Reynolds number
T	temperature, K
u	internal energy, $J\ kg^{-1}$
v	specific volume, $m\ kg^{-3}$
w	velocity with reference to free column cross-section, $m^3\ m^{-2}$
X	mass fraction
CCS	carbon capture and storage
DAE	differential and algebraic equation
DEPEG	dimethylether of polyethylene glycol
EoS	equation of state
IGCC	integrated gasification combined cycle
L/G	liquid-to-gas ratio
PC-SAFT	perturbed chain-statistical associating fluid theory
TR	test run

Subscripts

h	hydraulic
i,j	mixture component
in	inlet
L	liquid phase
P	particles
S	loading point
V	vapour phase

Greek letters

ϵ	void fraction, $m^3\ m^{-3}$
η	dynamic viscosity, $kg\ ms^{-1}$
	resistance coefficient
ρ	density, $kg\ m^{-3}$

dynamic operation is concerned. Transient performance of power plants is becoming extremely relevant, due to recent developments in the electricity market, namely the liberalization (in the European countries) and the increase of the share of electricity obtained from renewable energy sources. As a consequence, the IGCC power plant and the integrated capture unit have to be able to follow frequent and fast load changes in order to balance the intermittent nature of wind and/or solar radiation.

Dynamic process modelling and simulation is the state-of-the-art approach to improve the dynamic performance of such complex systems. Transient simulations can be of various use, for example, to test different control strategies including control parameter tuning (Casella and Colonna, 2012), to design startup and shutdown procedures (Dietl, 2012) as wells as emergency shutdown logics, and to study malfunction (Koch et al., 1999). The study described here focuses on dynamic modelling and simulation of load changes aimed at aiding the design of control strategies that can improve the dynamic performance of this type of plants. Startup and shutdown procedures are not treated because on the one hand they are considerably more complex, and on the other, overall improvement of dynamic performance due to an improvement of startup and shutdown operation is much less significant than that due to fast load changes.

In order to investigate the transient performance of the pre-combustion capture unit among others, a unique, fully instrumented CO_2 capture pilot plant has been realized at the Buggenum IGCC power station in the Netherlands by the utility company Vattenfall (Damen et al., 2011). Detailed dynamic models of the capture process have been developed by the authors and validated by comparison with transient experimental data obtained from the pilot plant. These validated models have been subsequently used in simulation studies on optimal control strategies in order to improve the process performance during load variations (Trapp et al., 2014; Trapp, 2014).

The study documented here focuses on the simulation and validation of one of the key components, the CO_2 absorber column with its auxiliaries. The literature treating the dynamic modelling and simulation of physical absorption for pre-combustion CO_2 capture is scarce. Heil et al. developed a dynamic model for a pre-combustion CO_2 removal unit utilizing methanol as solvent in an equilibrium-based absorber column model. The thermophysical properties of the fluid mixtures involved in the process are modelled with a simplistic approach (Heil et al., 2009).

A larger number of published studies is related to the dynamic performance of reactive absorption for post-combustion CO_2 capture, typically investigating the use of aqueous amine-based solvents (Chikukwa et al., 2012; Boot-Handford et al., 2014; Bui et al., 2014). This might be related to the fact that currently vari-ous post-combustion demonstration projects are ongoing, see, e.g., Ref. Wang et al. (2011). Moreover, the reactive absorption process is more challenging from the modelling point of view in com-parison to physical absorption. For adequate model predictions of multicomponent fluid processes involving chemical reactions, the more complex rate-based approach is required (Kucka et al., 2003; Lawal et al., 2009; Kale et al., 2013; Mac Dowell et al., 2013). Dif-ferent software tools have been identified as suitable for dynamic model development and simulation of chemical absorption for CO_2 capture (Ziaii et al., 2011; Prölß et al., 2011; Harun et al., 2012; Jayarathna et al., 2013). Specific model libraries are available in some commercial tools. Dietl developed an open source library according to a general modelling approach in order to allow for modelling of very different kinds of absorption and distillations processes (Dietl, 2012; Dietl et al., 2012).

Most of the dynamic models of post-combustion capture units were validated by comparison with steady-state experimental data (Lawal et al., 2010; Prölß et al., 2011; Harun et al., 2012; Jayarathna et al., 2013). Only few publications present transient measure-ment data obtained from pilot plant operation, mainly due to challenges in operating the CO_2 absorption plant in dynamic mode. Some authors treated the dynamic validation of the standalone CO_2 absorber model (Kvamsdal et al., 2011; Posch and Haider, 2013), while others validated the model by comparison with transient measurements related to the entire post-combustion capture unit, therefore including an integrated absorber and desorber column (Åkesson et al., 2011; Biliyok et al., 2012; Dietl, 2012). Accord-ing to the knowledge of the authors, an experimentally validated model (static or dynamic) of the physical absorption section of a pre-combustion CO_2 capture plant is not documented in the literature.

The notable aspects of this work are:

- Demonstration of an equation-based, object-oriented modelling approach using a non-proprietary modelling language, which is supported by various simulation environments (proprietary

and open source). The highly non-ideal fluid mixture properties are computed with accurate thermodynamic models, which have been validated against experimental data. These models are implemented, together with fast and robust algorithms, within an in-house property package, which is free for academic use. The open source model library containing the developed process models is available for academic purposes.

- Comprehensive dynamic model validation, whereby the absorber model and the model of the absorption and solvent regeneration section are validated by comparison with experimental data obtained from a pilot plant. Two transient tests have been performed, monitoring the response to step-wise changes of the syngas and solvent mass flow rate.

This paper is structured as follows: Section 2 briefly describes the CO_2 capture process, the applied modelling approach, the selected software tools and the model development focusing on the absorber column model. Section 3 covers the dynamic model validation of the standalone absorber model and subsequently the model of the absorption and solvent regeneration section. Concluding remarks are summarized in Section 4.

2. Model

2.1. Process description

This study is about the dynamic modelling of the absorption and solvent regeneration section of pre-combustion CO_2 capture units, however, for the sake of clarity, the entire capture process is shortly described. The simplified process flow diagram of the CO_2 capture pilot plant built at the site of the Buggenum IGCC power station is shown in Fig. 1. The configuration of the pilot plant is applicable to full-scale process plants, apart from few simplifications that are illustrated in the following.

The syngas from the gasifier entering the CO_2 removal unit is mixed with process water in order to obtain a pre-set steam/CO ratio, and thereafter the syngas–water mixture is fully evaporated and superheated by means of electrical heaters. Carbon monoxide present in the syngas is converted into hydrogen and carbon dioxide via a three-stage, sweet, high-temperature water–gas shift process. The excess process water is recovered from the shifted syngas through condensation and recycled. The shifted syngas, which contains about 35–40 mol% of CO_2, thereafter enters the absorption and solvent regeneration section. Carbon dioxide is removed from the syngas in a packed column by means of physical absorption utilizing the solvent dimethylether of polyethylene glycol (DEPEG) at process conditions corresponding to 40–45 °C and 21.5–22.5 bar. The resulting H_2-rich syngas is fed to the gas turbine of the com-bined cycle power plant and the CO_2 is recovered by three-stage depressurization of the loaded solvent. The lean solvent is recycled to the absorber, while the CO_2-rich product stream is compressed and in case of the pilot plant mixed again with the H_2-rich syn-gas. Typically, 80–85% of the CO_2 present in the shifted syngas is removed.

The design of a commercial-scale absorption and solvent regeneration unit is very similar to that of this pilot plant. The main difference is that the gas recovered from the first flash vessel (also called H_2 recovery vessel), which primarily contains co-absorbed hydrogen, is recompressed and recycled to the absorber column. This way the combustible H_2 is not lost with the CO_2 product.

2.2. Modelling approach

Dynamic system models for the aid of process and system design usually follow the lumped parameters approach, see, e.g., Ref. Cameron and Hangos (2001). Here models are based on first principles. Moreover the models are modular in order to master system complexity, i.e., the system is decomposed into suitable component models, which are connected through inter-faces representing physical boundaries. Typically zero-dimensional or one-dimensional component models were considered, as they provide a sufficient degree of detail for accurate predictions of the system performance, as shown in Section 3.

The models where implemented using the object-oriented, equation-based Modelica language (Fritzson, 2003). Modelica is a non-proprietary modelling language, which is supported by various commercial as well as open source simulation tools. Modelling features include reusability and extensibility, which allows for an easy adaptation of existing models.

2.3. Thermophysical properties

The thermophysical properties of the two-phase multi-component syngas–DEPEG mixture are calculated with the perturbed chain-statistical associating fluid theory (PC-SAFT) equation of state (EoS) (Gross and Sadowski, 2001) due to its success in

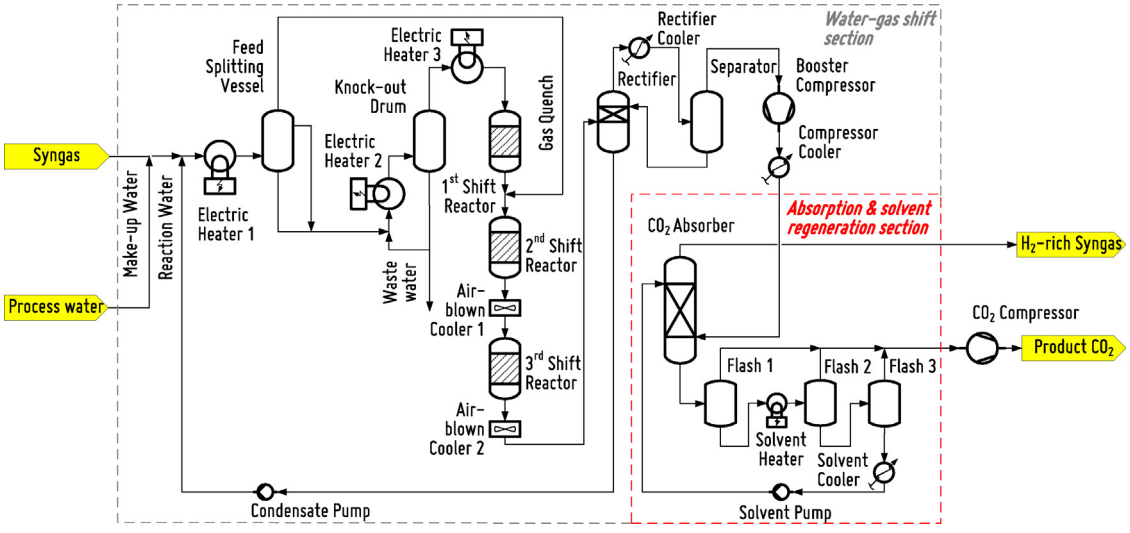

Fig. 1. Process flow diagram of the CO_2 capture pilot plant. The absorption and solvent regeneration section is highlighted in red. (For interpretation of the references to colour in this figure legend, the reader is referred to the web version of this article.)

predicting vapour–liquid equilibria of complex fluids and mixtures for a broad range of conditions. Moreover, due to the strong physical background and the small number of pure-component parameters, the PC-SAFT EoS is robust, consistent and extrapolative (Gross and Sadowski, 2001) even if calibrated on the basis of a limited amount of experimental thermodynamic property data.

The solvent DEPEG is employed in industry under the commercial names of Selexol^{TM} or Genosorb 1753^{TM}, whereby the latter one was tested in the pilot plant. For simplicity the sol-vent, which is a blend of glymes, is represented as a pseudo pure fluid in the thermodynamic model. The required pure-component parameters were obtained by fitting the EoS to published vapour pressure and liquid density data which is available for the lighter compounds of the blend (Nannan et al., 2013). The parameters of the heavier pseudo glyme were estimated by extrapolation following a method demonstrated by Nannan et al. (2013). In order to determine the binary interaction parameters, the PC-SAFT EoS was applied to experimental vapour–liquid equilibrium data pro-vided by the solvent vendor resulting in good agreement for binary mixtures between DEPEG and gases such as CO, CO_2, H_2, N_2, and water, if for the latter mixture cross-association interactions are considered (Nannan et al., 2013). The accuracy of the resulting thermodynamic model has proved to be suitable for engineering purposes. With regard to the transport properties, the liquid and vapour viscosity are predicted with the default models suggested for use together with the PC-SAFT EoS, see Ref. Aspen Technology (2013)

This EoS has been implemented, together with fast and robust algorithms, into an in-house property package (Colonna et al., 2004), which is interfaced with the dynamic modelling tool (Trapp et al., 2014). The use of external fluid property functions in Modelica process models puts some restrictions on the model development. Specific attention requires the formulation of the differential model equations, the choice of state variables and the causality of the system model. A detailed discussion of these modelling aspects is beyond the scope of this paper and the interested reader is referred to the publication of Trapp et al. (2014)

2.4. Dynamic absorber model

Models of physical absorption of gases into liquids differ in the way the mass transfer is treated (Taylor and Krishna, 1993). A simple representation of the phenomena is based on the assumption of thermodynamic equilibrium between the vapour and liquid phase. The more rigorous and accurate formulation accounts for the mass and heat transfer resistance between the phases, thus requiring rate equations. However, accuracy of the model predictions comes at the cost of model complexity and computational load. For dynamic process models, which are mathematically more complex than steady-state models, a reduction in degree of detail might be required in order to increase robustness and allow for reasonable simulation times. This applies especially to dynamic models used for plant-wide system analysis, such as it is the case for the absorption and solvent regeneration section model. This model is also intended for integration into the model of the entire CO_2 capture plant, and ultimately into the full power plant system model. Moreover, the aim of dynamic models is the accurate prediction of the transient performance and deviations in absolute values of process variables have often negligible impact on the prediction of the system dynamics.

The packed absorber column was therefore modelled following the equilibrium-based approach. The column is subdivided in theoretical stages assuming equilibrium between the vapour and liquid phase of the working fluid within each volume. Here, the number of equilibrium stages is tuned by comparison with the simulation results of a full rate-based model[1] in order to match steady-state performance at nominal operating conditions. When the absorber operation departs far from the design point less accurate steady-state performance estimates are then obtained with the equilibrium-based model. This behaviour is evaluated in the following.

Fig. 2(a) shows the percentage absolute deviation in CO_2 absorption efficiency[2] between the simulation results of the equilibrium-based and rate-based column model (operating range: syngas mass flow rate 800–1600 kg/h and solvent mass flow rate 10–18 kg/s). The comparison of the model predictions is also plotted in terms of CO_2 absorption efficiency as function of L/G ratio, see Fig. 2(b). Throughout the considered operating window deviations are smaller than 4.5% with a maximum at liquid-to-gas (L/G) ratio 22.5 and absorption efficiency 67.3%. In general, differences are higher at low L/G ratios corresponding to lower absorption efficiencies. Considering the observed differences in CO_2 absorption over the wide range of operating conditions, it can be argued that the equilibrium-based model describes the values of the main process variable with adequate accuracy for the aim of dynamic system simulations, whereby the interest is more on the correct estimation of transients.

It should also be considered that such an absorption and solvent regeneration unit is controlled based on the L/G ratio in order to maintain a constant extent of carbon capture. During transient operation it is therefore expected that the absorption efficiency does not deviate significantly from its design value and hence a well-tuned equilibrium-based model is sufficient to describe the transient performance. Section 3 describes the verification of this model assumption by means of model validation against experimental data.

In general, a dynamic process model is described by conservation and constitutive equations typically resulting in a set of differential and algebraic equations (DAE's), which can be classified according to its index (Lötstedt and Petzold, 1986; Unger et al., 1995). It is numerically difficult to solve high-index DAE systems and therefore current simulation tools implementing the Modelica language employ state-of-the-art techniques for index reduction. However, difficulties related to index reduction operations might arise in case external functions, such as those providing fluid property estimations, are needed within the process models (Trapp et al., 2014).

In order to keep the index of the DAE system as low as possible, the modelling procedure described, e.g., in Refs. (Casella et al., 2008; Casella and Colonna, 2012) has been adopted. It can be synthetically explained as follows:

- The model of each component is first discretized into so-called resistive (zero volume approximation) and storage modules (zero potential drop approximation), thus solving the conservation law equations for the generalized flow variable within the resistive module, and for the generalized potential variable within the storage module.
- Resistive modules are then connected to storage modules to form components, and such causality is used to connect components to form the system model.

Based on this modelling procedure, the stage-wise discretized packed column with counter-current flow of vapour and liquid can

[1] The performance of the absorber column is obtained by a rigorous, rate-based model for simulating all types of multi-stage, vapour–liquid fractionation operations under steady-state operating conditions (Aspen Technology, 2013).

[2] The CO_2 absorption efficiency is defined as the molar flow rate of absorbed CO_2 in the rich solvent leaving the absorber divided by the molar flow rate of CO_2 in the syngas entering the column.

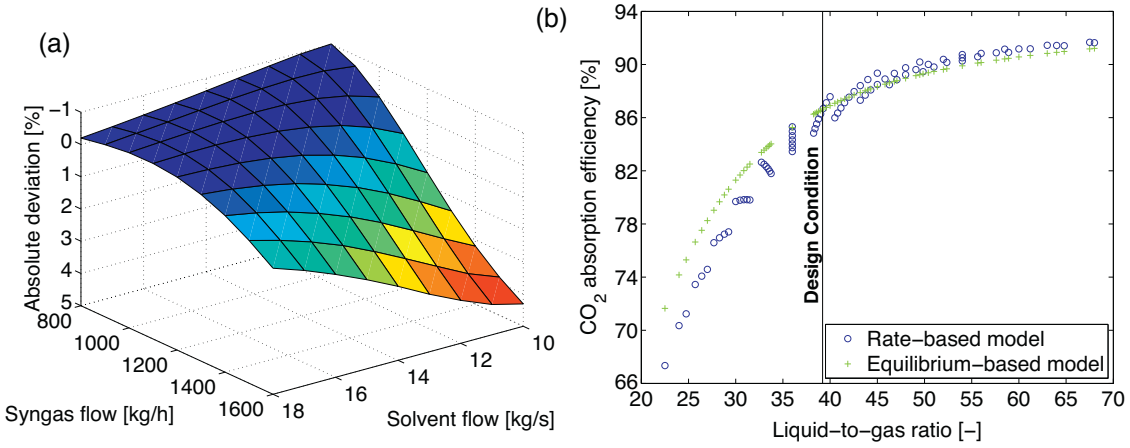

Fig. 2. Comparison of steady-state simulation results obtained with the equilibrium- and the rate-based models. (a) Absolute deviation[3] of the prediction of CO_2 absorption efficiency. (b) CO_2 absorption efficiency for different liquid-to-gas ratios.

be represented as a series of equivalent tray modules (storage module) and valve or liquid head modules (resistive module).

Within the equivalent tray module, pressure, temperature and composition of the liquid and vapour phase are determined by solving the conservation equations for mass and energy, assuming thermodynamic equilibrium between liquid and vapour. The component mass and energy balance read

$$\frac{dM}{dt}X_\mathrm{i} + M\frac{dX_\mathrm{i}}{dt} = m_\mathrm{Lin}X_\mathrm{Lin,i} + m_\mathrm{Vin}X_\mathrm{Vin,i} - m_\mathrm{Lout}X_\mathrm{Lout,i} - m_\mathrm{Vout}X_\mathrm{Vout,i}, \quad (1)$$

$$M\frac{du}{dt} + u\frac{dM}{dt} = m_\mathrm{Lin}h_\mathrm{Lin} + m_\mathrm{Vin}h_\mathrm{Vin} - m_\mathrm{Lout}h_\mathrm{Lout} - m_\mathrm{Vout}h_\mathrm{Vout}, \quad (2)$$

where M, u, X_i are the total mass, internal energy and component mass fraction of the fluid within the volume of the tray. For reasons of computational efficiency the vessel pressure p, temperature T and overall mass fraction X_i are selected as state variables. Hence, the mass and energy balance need to be expressed in terms of the state derivatives $\frac{dp}{dt}$, $\frac{dT}{dt}$ and $\frac{dX_\mathrm{i}}{dt}$, yielding

$$\frac{dM}{dt} = -M\rho\left[\left(\frac{\partial v}{\partial p}\right)_{T,X}\frac{dp}{dt} + \left(\frac{\partial v}{\partial T}\right)_{p,X}\frac{dT}{dt} + \sum_{i=1}^{n}\left(\frac{\partial v}{\partial X_\mathrm{i}}\right)_{p,T,X_\mathrm{j\neq i}}\frac{dX_\mathrm{i}}{dt}\right], \quad (3)$$

$$\frac{du}{dt} = \left(\frac{\partial u}{\partial p}\right)_{T,X}\frac{dp}{dt} + \left(\frac{\partial u}{\partial T}\right)_{p,X}\frac{dT}{dt} + \sum_{i=1}^{n}\left(\frac{\partial u}{\partial X_\mathrm{i}}\right)_{p,T,X_\mathrm{j\neq i}}\frac{dX_\mathrm{i}}{dt}. \quad (4)$$

The required thermodynamic properties, including the partial derivatives of fluid thermodynamic properties, are obtained from the external thermophysical property library as $prop = prop(p, T, X_\mathrm{i})$.

The momentum equation pertaining to the resistive module is substituted by empirical correlations to describe the hydrodynamics of the stage predicting the liquid and vapour flow rate as a function of the pressure difference between the stages, the liquid holdup and the packing characteristics. The pressure drop Δp is calculated with empirical correlations of Billet and Schultes (1999), thus

$$\frac{\Delta p}{H} = \psi_\mathrm{L}\frac{a}{(\epsilon - ho_\mathrm{L})^3}\frac{F_\mathrm{V}^2}{2}\frac{1}{K}, \text{ and} \quad (5)$$

$$\psi_\mathrm{L} = C_\mathrm{p}\left(\frac{64}{Re_\mathrm{V}} + \frac{1.8}{Re_\mathrm{V}^{0.08}}\right)\left(\frac{\epsilon - ho_\mathrm{L}}{\epsilon}\right)^{1.5}\left(\frac{ho_\mathrm{L}}{ho_\mathrm{L,S}}\right)^{0.3} \exp\left(C_1\sqrt{Fr_\mathrm{L}}\right) \quad \text{with } C_1 = \frac{13300}{a^{3/2}}. \quad (6)$$

The pilot plant absorber is operated in the pre-loading region, therefore the liquid holdup equals the holdup at the loading point: $ho_\mathrm{L} = ho_\mathrm{L,S}$. The liquid holdup ho_L is given by Billet and Schultes (1999)

$$ho_\mathrm{L} = \left(12\frac{1}{g}\frac{\eta_\mathrm{L}}{\rho_\mathrm{L}}w_\mathrm{L}a^2\right)^{1/3}\left(\frac{a_\mathrm{h}}{a}\right)^{2/3}, \text{ with} \quad (7)$$

$$Re_\mathrm{L} = \frac{w_\mathrm{L}\rho_\mathrm{L}}{a\eta_\mathrm{L}} \geq 5 : \frac{a_\mathrm{h}}{a} = 0.85C_\mathrm{h}Re_\mathrm{L}^{0.25}\left(\frac{w_\mathrm{L}^2 a}{g}\right)^{0.1}. \quad (8)$$

Storage of thermal energy in the packing is considered, however heat losses to the environment are neglected.

Based on the implemented model equations, various model parameters have to be specified related to the column geometry and the characteristics of the packing. These parameters and the related values applicable to the pilot plant absorber are given in Table 1. Transport properties such as dynamic viscosity of the liquid and vapour phase are assumed constant and mean values are used based on the absorber operating point (Aspen Technology, 2013).

2.5. Additional process models and control

For the modelling of the entire absorption and solvent regeneration section, additional process models for the absorber sump, the flash vessels, the solvent cooler and solvent pump are necessary (see Fig. 1). These models are documented in a related paper dealing with the dynamic modelling and simulation of the entire CO_2 capture unit (Trapp et al., 2014). The system model is obtained by assembly of the individual component models and adjustment of the geometrical data. Equipment sizing information of the pilot plant components is summarized in Table 1.

[3] The absolute deviation of CO_2 absorption efficiency is defined as the difference between the prediction of the equilibrium-based and rate-based model divided by the estimation of the rate-based model.

Table 1
Model parameters of main pilot plant components.

Parameter description	Value
Number of theoretical absorber stages	3
Absorber column diameter d	0.76 m
Absorber packing height H	9.4 m
Packing type	Raschig Super-Pack 250Y
Packing specific surface area a	250 m^2 m^{-3}
Void fraction ϵ	0.98 m^3 m^{-3}
Constant for pressure drop correlation C_p	19.5[b] (default 0.18[a])
Constant for holdup correlation C_h	0.65 [a]
Packing density	310 kg m^{-3}
Packing specific heat capacity	500 J kgK^{-1}
Absorber sump diameter	0.76 m
Absorber sump height	9.3 m
1st flash vessel volume	5.6 m^3
2nd flash vessel volume	2.4 m^3
3rd flash vessel volume	2.4 m^3

[a] Provided by packing supplier.
[b] Adjusted to foster numerical convergence.

In addition, for dynamic process simulations, an appropriate control scheme is required. That entails in this case the modelling of linear valves and PI controllers. The pilot plant control scheme is thus included in the dynamic system model. The individual control loops are summarized in Table 2 and depicted in the object diagrams of the dynamic models presented in Section 3. For a large-scale plant, the capture rate is typically maintained by a L/G ratio controller, which was however not implemented in the pilot plant. Other critical control parameters are those influencing the absorption of CO_2. These are the pressure in the absorber column, the temperature of the lean solvent and the pressure of the low-pressure flash vessel.

The basic component models such as sinks, sources, valves, pres-sure drops and pumps are taken from the ThermoPower library (Casella and Leva, 2006, 2005) and adapted in terms of their work-ing fluid models which have been replaced with functional calls to the external property tool in order to accurately estimate the property values of the syngas–DEPEG mixture.

3. Dynamic validation

Two types of dynamic experiments were performed at the Buggenum CO_2 capture pilot plant for model validation purposes: During the first tests (TR-Solvent), the solvent mass flow rate was changed stepwise, while keeping the syngas mass flow rate, the water content in the solvent, the absorption pressure and temperature constant. In the second tests (TR-Syngas), the syngas mass flow rate was perturbed stepwise, while maintaining unchanged the values of the other input variables. Both types of experiments cause transient changes of the liquid-to-gas flow ratio, which has a large impact on the process performance, e.g., on the CO_2 capture

Table 2
Absorption and solvent regeneration section control loops.

Process variable	Control variable	Set point
Absorber column pressure	Opening H_2-rich gas flow valve	21.7 bar
1st flash vessel pressure	Opening 1st flash vessel gas flow valve	7.5 bar
2nd flash vessel pressure	Opening 2nd flash vessel gas flow valve	2.9 bar
Absorber sump level	Opening rich solvent flow valve	2000 mm
1st flash vessel level	Opening 1st flash vessel liquid flow valve	2000 mm
3rd flash vessel level	Opening 2nd flash vessel liquid flow valve	800 mm
Solvent mass flow rate	Opening lean solvent flow valve	15 kg/s
Lean solvent temperature	Opening cooling water flow valve	40 °C

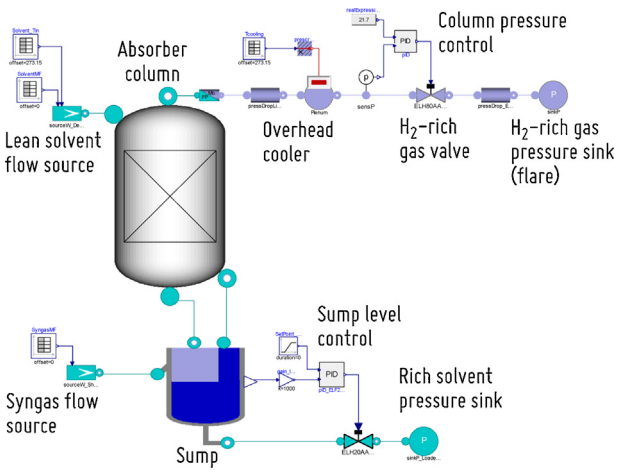

Fig. 3. Object diagram of the system model used for the absorber validation.

efficiency. These tests are expected to be suitable for the validation of the predictive capabilities of the models.

First, the validation of the standalone absorber model is discussed in detail and afterwards the validation of the absorption and solvent regeneration section model is presented.

3.1. Absorber model validation

The purpose of the dynamic tests is to obtain data for the qualitative and quantitative validation of the transient performance of the process model. Regarding the absorber column, the holdup in the liquid and vapour phase is the main process variable which determines the dynamic system response. Hence, the experimental data are used to qualitatively validate the correct choice of the holdup correlation, see Eqs. (7) and (8). Note that the adopted correlation is commonly used for higher gas capacity factors than observed in the pilot plant (Billet and Schultes, 1999). The hydrodynamic coefficient of the holdup correlation C_h can be tuned in order to achieve good agreement between model predictions and measurements. For the test run results presented in this paper tuning of the hydrodynamic coefficient was not necessary and the default value was used throughout all simulations. The measured process variables used for the quantitative absorber model validation are volumetric flow rate, temperature, CO_2 and H_2 composition of the H_2-rich gas, absorber pressure and column pressure drop.

The object diagram of the system model used for the absorber validation is illustrated in Fig. 3. The model comprises the absorber column and sump, a flow source for the syngas and the lean solvent, the sump level control, a pressure sink for the rich solvent, a pressure drop representing frictional losses of the H_2-rich gas in the overhead cooler, a gas tank representing storage of mass in the overhead cooler, the H_2-rich gas control valve including the absorber pressure PI controller, a quadratic pressure drop representing the frictional losses in the piping delivering the H_2-rich gas to the flare and a pressure sink representing the flare.

The friction coefficient for the linear pressure drop of the overhead cooler was fitted to experimental data in order to match outlet pressures for on- and off-design steady-state operation. The friction coefficient of the quadratic pressure drop of the piping to the flare was tuned in a similar way in order to match pressures and the valve opening.

Inputs of the model which fluctuate or change during the transient and influence the transient response of the system are chosen as prescribed variables. These are: syngas mass flow rate, solvent mass flow rate, solvent inlet temperature and the overhead cooler outlet temperature. The overhead cooler has not been modelled

Table 3
Process condition of syngas and lean solvent stream.

Process variable	Shifted syngas	Lean solvent
Pressure [bar]	22[a]	22[a]
Temperature [°C]	40	40[b]
Mass flow rate [kg/s]	0.39[b]	15[b]
Mole fraction		
CO	0.024	5 ppm
H_2	0.546	30 ppm
CO_2	0.375	0.031
H_2O	0.004	0.106
N_2	0.051	30 ppm
DEPEG	0	0.862

[a] Initial start value. The actual value is an output of the simulation.
[b] Initial steady-state value. This variable is a prescribed variable for the dynamic model, hence measurements are used as input.

due to lack of measurement data. The other input variables such as syngas temperature, rich solvent pressure and flare pressure remain constant during the transient operation.

The process measurements are obtained from the distributed control system of the pilot plant and are transferred for off-line data analysis to suitable data processing tools. Measurements are recorded when changes in variable values exceed a threshold which was set for most of the variables to 0.1% of the individual measurement range. All instruments were calibrated either on-site or at the production facility typically at nominal operating conditions. The measurement uncertainty is estimated with about 1% for most of the instruments.

Open-loop tests (i.e., control system not in operation) are most suitable in order to validate that the process dynamics are captured correctly by the dynamic model. However, open-loop tests cannot be performed safely on the absorption and solvent regeneration unit. Partial open-loop test were therefore designed, in which only control loops which do not compromise the safe and stable operation were put into manual mode. The transient of such disturbance rejection experiments is thus the result of the interaction between the process dynamics and the inherent control loop dynamics and primarily provides relevant dynamic information in the frequency range around the controller's crossover frequency. The evaluation of measured and predicted dynamics is based on the main transient parameters such as time and value of maximum overshoot, settling time, frequency and damping of oscillations.

3.1.1. Change in solvent mass flow rate (test run TR-Solvent)

The process conditions of the syngas and lean solvent flow are summarized in Table 3. During this experiment, the mass flow control valve of the solvent was manually changed without the solvent flow controller in operation. The perturbations to the valve open-ing correspond to changes in solvent flow of 2, 4 and 5 kg/s. The validation is performed with process data acquired during the test in which the solvent mass flow rate was increased from 10 kg/s to 15 kg/s. This is an upward step from off-design to the nomi-nal operating condition, therefore the initial steady-state values predicted by the model might deviate somewhat from the experimental values. The change in solvent mass flow rate is depicted in Fig. 4(a).

The syngas mass flow rate, which is a prescribed variable for the dynamic model, is shown in Fig. 4(b). The opening of the valve controlling the syngas mass flow is maintained constant during the test in order to keep the syngas flow constant. However, during the change of the absorber column pressure, which is the same as the back pressure to the syngas control valve, the syngas mass flow varies. Though, the syngas flow changes are relatively small compared to the changes in solvent flow.

Considering the absorber pressure response depicted in Fig. 4(c), the stepwise increase in solvent mass flow rate initially results in a column pressure increase. The pressure control opens the valve in order to maintain the pressure set point. Subsequently, the pressure decreases again and reaches its set point value after a few oscilla-tions. The increase in solvent flow rate enhances CO_2 absorption resulting in a lower H_2-rich gas flow, which leads to a decrease of the pressure drop over the overhead cooler. The final steady-state column pressure is therefore slightly lower as the pressure is controlled downstream of the overhead cooler.

First, the performance of the pressure control loop is analyzed by considering the transient of the pressure at the top of the absorber column (process variable), the opening of the H_2-rich gas flow valve (control variable) and the H_2-rich volumetric flow rate, which are depicted in Fig. 4(c)–(e) respectively. It can be observed that the frequency and damping of the oscillations, which are determined by the dynamic interaction of the controller and process dynamics, are well matched by the simulation. Thus, the dynamic influence of the control variable on the controlled variable is captured correctly in the frequency range which is relevant for the closed-loop performance, i.e., around the crossover frequency (about 0.016 rad/s).

The process response to the applied disturbance on the other hand is overestimated during the initial part of the transient, where the model predicts a much larger change than observed in the experimental measurements. For example, the initial pressure peak is predicted to be 3 times larger than measured. Thereafter, however, deviations are rather small. This means that the high-frequency response of the model is overestimated, compared to reality. This is probably due to some neglected phenomenon which has a damping action on the effect of the disturbance. At the top of the absorber column, a liquid distributor is located, which can store liquid in the order of 100 l and thus delay fast transient changes in the solvent flow. This liquid distributor is not included in the dynamic model. The more aggressive variable changes predicted by the simulation might therefore be explained by the fact that storage occurs in the distributor particularly during the initial tran-sient which is not modelled. Another possible explanation might be due to the fact that the absorber is modelled as the connection of a finite number of volumes at thermodynamic equilibrium, while the real process is a continuum of non-equilibrium mass and energy transfer phenomena, which might react more slowly to this kind of disturbance.

As far as steady-state values are concerned, the model under-predicts the initial off-design value of the H_2-rich flow and consequently the opening of the valve. This deviation to the measured flow value, which is in the order of 4%, is related to the fact that, at L/G ratios much smaller than the ratio at the design point, the equilibrium-based model overpredicts the absorption efficiency (see Section 2.4). However, the accuracy of the prediction of dynamic indicators is not affected by this deviation.

In the following the results of the pressure drop of the absorber packing is discussed. The adopted Billet and Schultes pressure drop correlation includes the friction coefficient C_p, which can be tuned in order to match the measured pressure drop over the column. As the dynamic pressure drop of the two column packings is not measured individually but lumped with the frictional losses of the liquid distributors, a fitting of the measured values to determine the friction coefficient is not meaningful. Moreover, due to numerical instabilities of the simulations in case of small dynamic pressure drop, the friction coefficient was adjusted such that the overall column pressure drop is approximately 20 mbar. Such a relatively high value of the dynamic pressure drop significantly enhances the robustness of the simulations. This value is similar to the total pres-sure loss measured in the absorber column at nominal operating conditions, which includes the dynamic pressure drop and the dis-tributor losses. In general, the pressure drop does not affect the dynamics of the absorber column model in terms of heat and mass

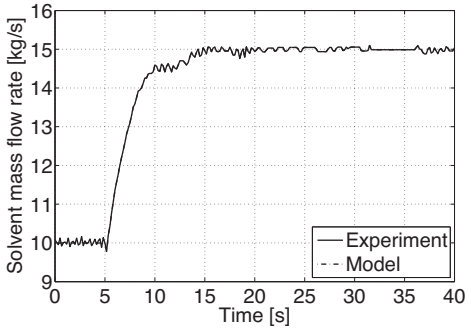

(a) Solvent mass flow rate (model input).

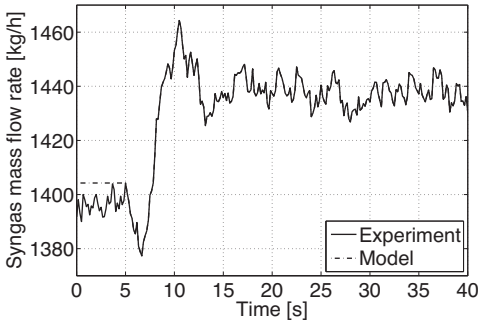

(b) Syngas mass flow rate (model input).

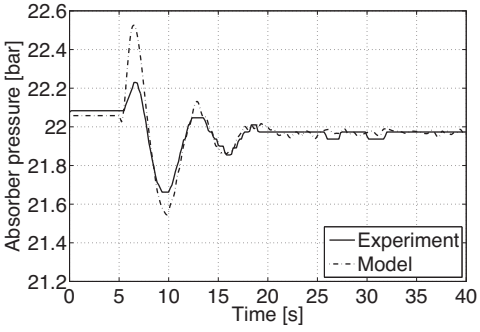

(c) Pressure at the top of the absorber column.

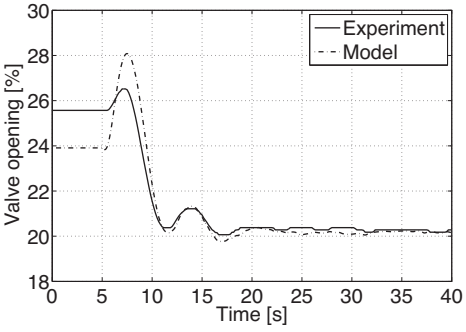

(d) Percentage opening of the H_2-rich gas valve.

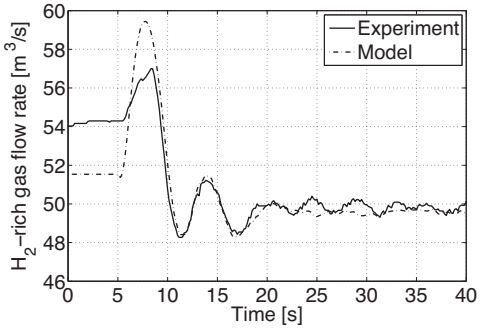

(e) H_2-rich gas volumetric flow rate.

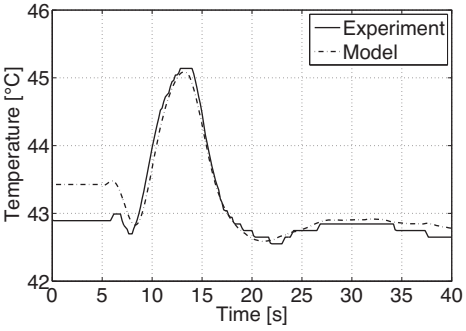

(f) Gas temperature between the packings.

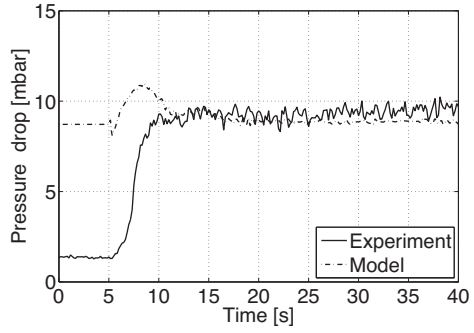

(g) Pressure drop over the first packing.

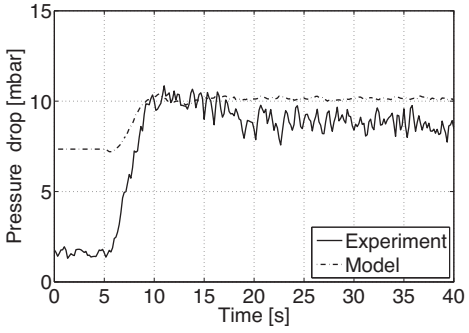

(h) Pressure drop over the second packing.

Fig. 4. TR-Solvent: comparison of measurements and simulation results.

transfer, hence the adjustment of the pressure drop for numerical reasons is justified.

The comparison of the time-dependent measurements and model predictions of the pressure drop over the first and the second packing are visualized in Fig. 4(g) and (h). The first pack-ing is situated at the upper part of the column and the second below.

The transient of the working fluid pressure drop over the first packing is not predicted correctly. The model predictions only depend on the solvent and syngas volumetric flow rate and the densities of the vapour and liquid (see Billet and Schultes pressure drop correlation Eqs. (5) and (6)), while the pressure loss induced by the liquid distributor situated above the packing is not modelled. This might be the main reason of the discrepancy

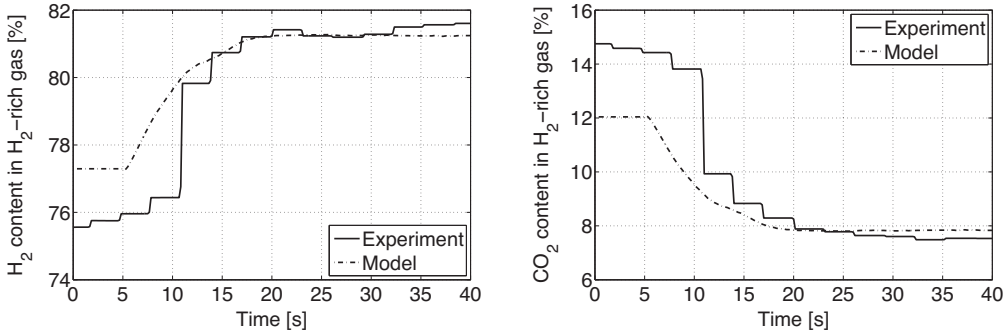

(a) H_2 content in H_2-rich gas flow. (b) CO_2 content in H_2-rich gas flow.

Fig. 5. TR-Solvent: comparison of measurements and simulation results.

between measured and simulated values. The model predicts an initial increase of the pressure drop caused by the step increase in solvent mass flow rate. The pressure drop successively decreases and returns approximately to its initial value, which is explained by the delayed decrease of the H_2-rich gas flow associated with a lower frictional loss due to the increase of CO_2 absorption.

The model correctly predicts the pressure transient of the work-ing fluid experienced by the second packing. However, the absolute change in pressure drop is underpredicted, which is explained by the fact that the redistributor situated above the second bed is not represented in the model. Inspection of Fig. 4(h) shows that the pressure drop due to flow friction within the second packing increases with increasing solvent flow rate. Moreover, the gas flow
rate variation due to enhanced CO_2 absorption is smaller within the second packing than the first. It can therefore be concluded that the pressure drop variation depends mainly on the solvent mass flow rate.

Due to the fact that measurements and simulation results of the pressure drop represent different phenomena (dynamic pres-sure drop and distributor losses versus adjusted dynamic pressure drop), the steady-state values will in principle not match. The friction coefficient of the dynamic model has however been adjusted such that a reasonable agreement is achieved for the final steady-state values at nominal condition.

Fig. 4(f) presents the comparison of measurements and model results for the response in gas temperature between the packings. The gas temperature temporarily increases caused by fluctuations in the lean solvent temperature, which is therefore applied as a prescribed variable for the dynamic model. The transient model predictions show good agreement with the measurements.

Finally, Fig. 5(a) and (b) depicts the measured H_2 and CO_2 content in the H_2-rich gas flow as function of time, together with their model-based predictions. The simulation results compare well with the experimental data, except for an initial time delay in the mea-surements. In this respect, it is important to mention that the mixture composition is not measured continuously but values are recorded every three minutes. Time delays for sampling and composition analysis are only approximately known (about 300 s) and have already been corrected for in the comparison. The initial delay that can be observed in the recorded values cannot therefore fully be explained. The difference between the predicted and measured initial transient might, however, be attributed to the assumption of thermodynamic equilibrium for the absorber model.

As far as initial steady-state values are concerned, the model overpredicts the value of H_2 content and underpredicts the value of CO_2 content. This is attributed to the overprediction of the CO_2 absorption efficiency by the equilibrium-based model at this off-design operational point (see Fig. 2).

3.1.2. Change in syngas mass flow rate (test run TR-Syngas)

During the test run TR-Syngas, manual step changes were applied to the back pressure control valve of the upstream syngas compressor without the pressure control in operation. The validation is performed with the data recorded during the experiment in which the syngas mass flow rate was decreased from 1400 kg/h to 800 kg/h. Differently from the TR-Solvent test run, this is a down-ward step from the nominal operating condition to an off-design condition. The change in syngas mass flow rate is depicted in Fig. 6(b).

The set point of the lean solvent mass flow controller was kept constant during the transient in order to maintain the flow rate. However, the solvent mass flow rate fluctuates slightly, by less than 1.5 % (see Fig. 6(a)). These fluctuations are due to changes in the absorber column pressure during the test. Since the absorber column pressure is the same as the back pressure to the solvent control valve, the solvent flow controller needs to adjust. Therefore, the solvent flow rate is set as prescribed variable for the dynamic model.

For the absorber pressure, the step decrease in syngas mass flow rate results in a drop of the column pressure. Subsequently, the pressure controller adjusts the opening of the H_2-rich gas valve to return to the given pressure set point. As a result, the pressure increases again and reaches its final steady-state condition after a few oscillations. The final steady-state value is slightly lower than its initial value. As explained for the validation of the test run TR-Solvent, this off-set is related to the decrease in H_2-rich gas flow rate.

The predicted and measured transient of the variables related to the pressure control loop are compared in Fig. 6(c) – pressure at the top of the absorber column, in Fig. 6(d) – opening of the H_2-rich gas flow valve, and in Fig. 6(e) – H_2-rich volumetric flow rate. Excellent agreement is achieved between the model and the experiments for the closed-loop performance, i.e., the dynamic interaction of the controller and process dynamics, and for the process response to the disturbance.

In comparison to the test run TR-Solvent, the model predictions for the pressure control loop are significantly better, in particu-lar considering the initial transient. While during TR-Solvent the damping action of the liquid distributor might have effected the disturbance, this phenomenon is not relevant for TR-Syngas and might therefore explain the much better agreement. It is also worth pointing out that the perturbation of the syngas mass flow rate dur-ing TR-Syngas is a ramp with a duration of approximately 600 s, whereas the ramp duration of TR-Solvent is roughly 300 s. This might indicate that the model predictions are less accurate for high-frequency response, possibly due to the use of an equilibrium-based absorber column model.

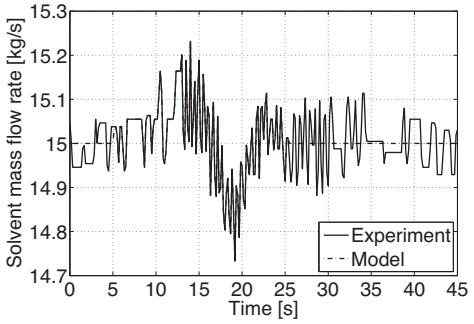

(a) Solvent mass flow rate (model input).

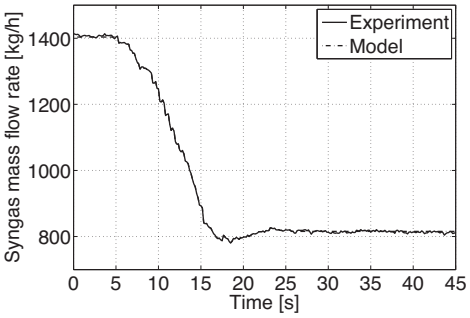

(b) Syngas mass flow rate (model input).

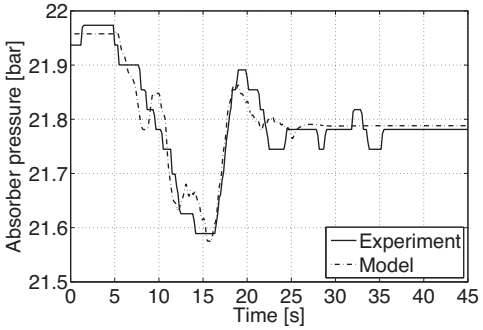

(c) Pressure at the top of the absorber column.

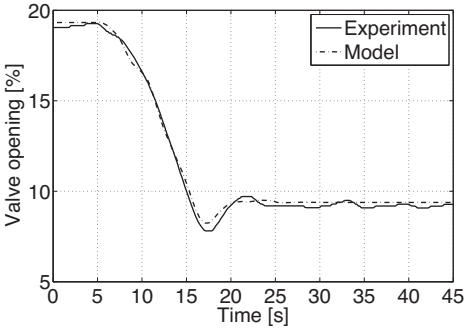

(d) Percentage opening of the H_2-rich gas valve.

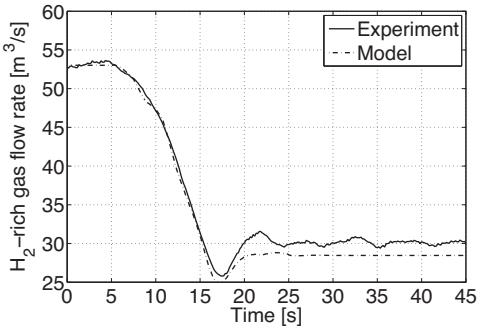

(e) H_2-rich gas volumetric flow rate.

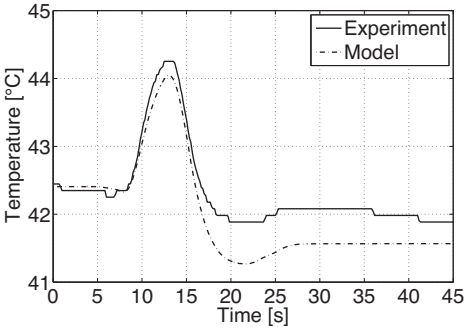

(f) Gas temperature between the packings.

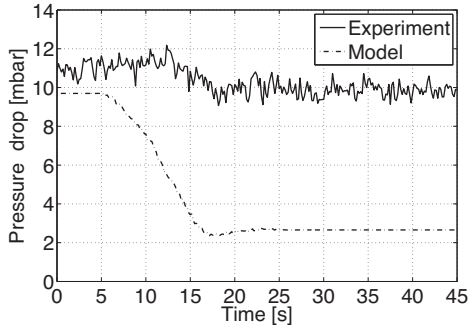

(g) Pressure drop over the first packing.

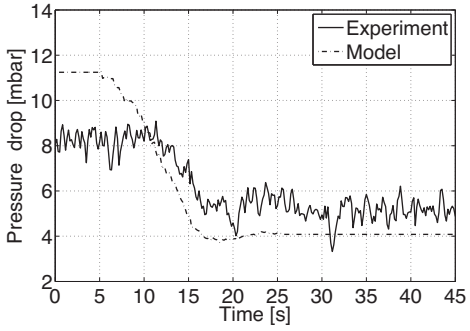

(h) Pressure drop over the second packing.

Fig. 6. TR-Syngas: comparison of measurements and simulation results.

As far as steady-state values are concerned, the model accurately predicts the initial and final steady-state values of the variables related to the absorber pressure control. The largest deviations are observed for the off-design value of the H_2-rich gas flow.

Fig. 6(g) and (h) visualizes the comparison of the experimental data and model predictions for the pressure drop over the first and second packing. For both packings the transient response, a decrease in pressure drop caused by a decrease in vapour flow, is predicted correctly. The change in vapour flow has two reasons: first the decrease in entering syngas flow and second the decrease in H_2-rich product flow as a result of enhanced CO_2 absorption.

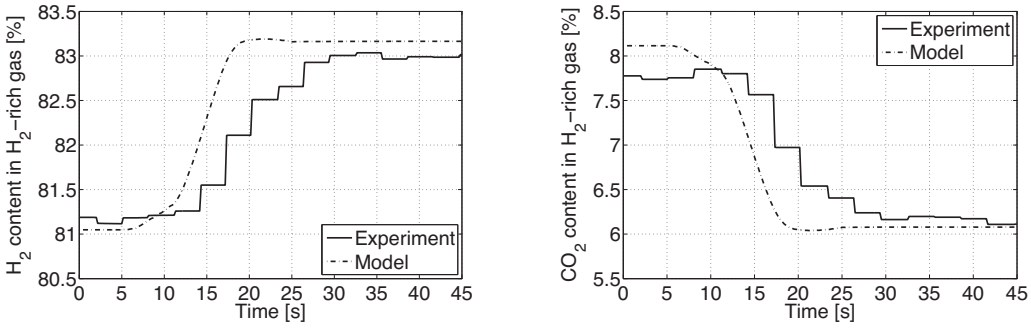

(a) H_2 content in H_2-rich gas flow. (b) CO_2 content in H_2-rich gas flow.

Fig. 7. TR-Syngas: comparison of measurements and simulation.

The absolute values for the initial and final steady-state pressure drops are not predicted correctly. As explained for TR-Solvent, the pressure drop of the liquid distributors above the first and second bed are not modelled and therefore measured losses cannot be compared with model predictions which only represent the dynamic pressure drop.

During test run TR-Syngas, the solvent mass flow rate and there-with the pressure drop of the liquid distributors remained almost constant. Hence, the change in pressure drop is mainly related to the variation in vapour flow. Consequently, the absolute change in pressure loss could be used to tune the friction coefficient of the adopted pressure drop correlation in order to match experimental data. However, this fitting was not performed as it was required to adjust C_p in order to improve the numerical robustness of the simulation (see discussion for test run TR-Solvent).

Fig. 6(f) shows the measurements and model predictions for the transient of the gas temperature between the packings. The temporary increase in gas temperature is caused by fluctuations in the lean solvent temperature which is thus defined as prescribed variable. The model predictions show good agreement with the experimental data. The observed deviations in the final steady-state are approximately 0.5 °C. Finally, Fig. 7(a) and (b) show the compar-ison of the experimental data and model predictions for the H_2 and CO_2 content in the H_2-rich gas flow. With a decrease in syngas mass flow at constant solvent flow rate, the CO_2 absorption efficiency increases which leads to a lower CO_2 content and higher H_2 content in the H_2-rich product flow. The transient response as well as the steady-state values are predicted correctly. A slight time delay is observed in the measurements similar to experiment TR-Solvent.

To summarize, with respect to model performance for the steady-state values of the main process variables, excluding the packing pressure drop, the following conclusions can be drawn: (a) at on-design operation (L/G = 38.6) the variable values are reproduced with an error of less than 1% and (b) at off-design operation (L/G = 67.5 & 25.7) the values are reproduced with less than 5% error. These results can be considered as satisfactory, keeping in mind that the latter deviations are related to the equilibrium assumption (see Fig. 2).

Considering the main dynamic parameters of the observed transients of absorber pressure and temperature, H_2-rich gas flow rate and composition, namely, time and value of maximum overshoot, settling time, frequency and damping of oscillations, then these parameters are predicted with less than 15% error; larger deviations are observed during the initial transient of TR-Solvent related to the fact that a possible delay in solvent flow variation is not modelled. In general, this agreement between the experimental data and model predictions can be considered as satisfactory.

The transient and the absolute values of the column pressure drop over the first and second packing is in most cases not predicted correctly due to the fact that the frictional losses of the distributors are not modelled. In addition, agreement in the absolute values is not achieved because the friction coefficient C_p had to be adjusted in order to enhance numerical robustness of the simulations.

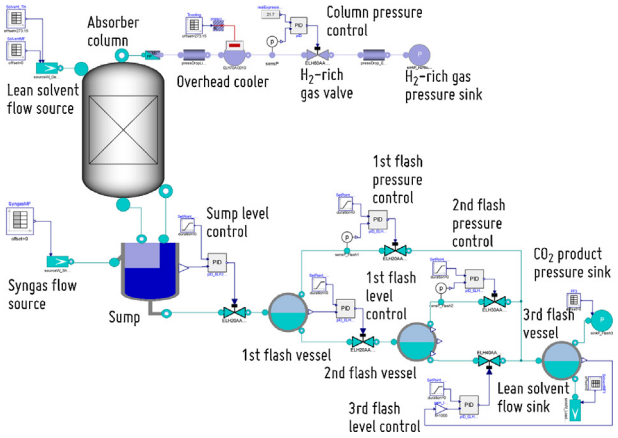

Fig. 8. Object diagram of the system model used for validation of the absorption and solvent regeneration section.

3.2. *Absorption and solvent regeneration section model validation*

After validation of the standalone absorber model, the model of the absorption and solvent regeneration section was validated. The process variables used for the quantitative comparison of the transient performance of the model with the recorded measurements are the volumetric vapour flow rates and pressures of the three flash vessels, and the CO_2 and H_2 composition of the 3rd flash (see Fig. 1).

The object diagram of the absorption and solvent regeneration section model used for validation is depicted in Fig. 8. Here, the model of the absorber (see Fig. 3) is extended with three flash vessels, two gas control valves with PI pressure controller and two liquid control valves with PI level controller, a CO_2 product pressure sink and a lean solvent flow sink. For ease of validation the solvent recycle was kept open in the system model. In the solvent regeneration section, the pressure of the 3rd flash vessel and the lean solvent flow leaving the 3rd flash are applied as prescribed variables.

3.2.1. *Change in syngas mass flow rate*

The validation was performed using the experimental results of test run TR-Syngas, in which the syngas mass flow rate was changed stepwise from 1400 kg/h to 800 kg/h, see Fig. 6(b). As response to the decrease in syngas flow rate, it is expected that the vapour

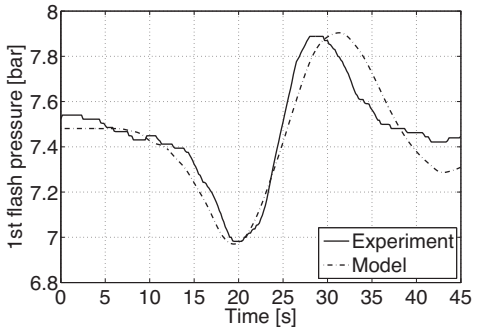

(a) 1st flash pressure.

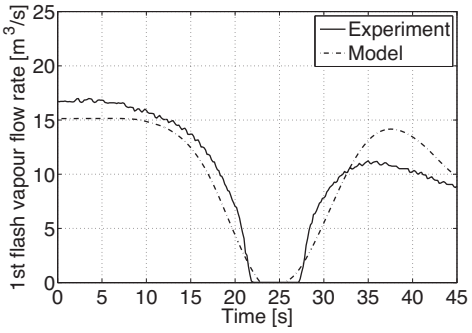

(b) 1st flash volumetric vapour flow rate.

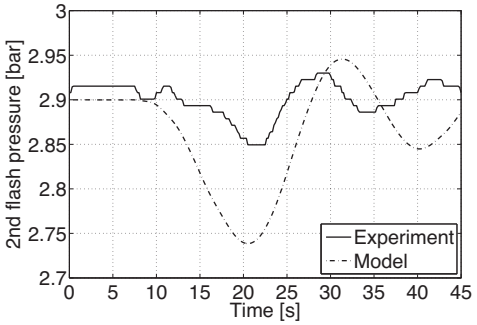

(c) 2nd flash pressure.

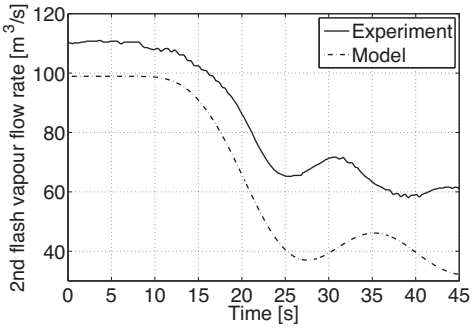

(d) 2nd flash volumetric vapour flow rate.

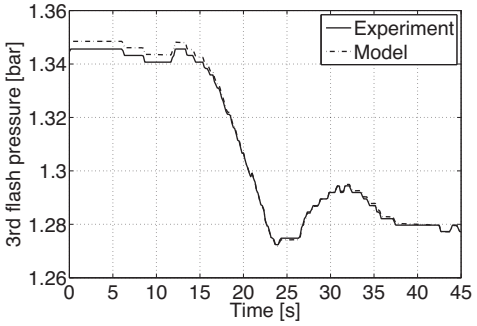

(e) 3rd flash pressure (model input).

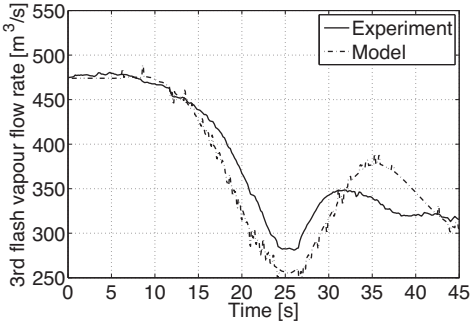

(f) 3rd flash volumetric vapour flow rate.

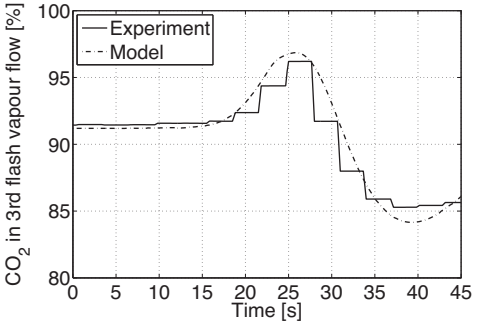

(g) CO_2 content in 3rd flash vapour flow.

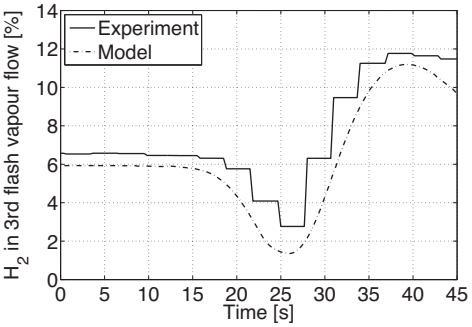

(h) H_2 content in 3rd flash vapour flow.

Fig. 9. TR-Syngas: comparison of measurements and simulation results.

flow rates at the flash vessels decrease. Subsequently, the vessel pressures drop initially and the pressure controllers act in order to maintain the pressure set points.

The experimental data and simulation results of the dynamics of the pressures and volumetric vapour flow rates of the three vessels are compared in Fig. 9. It can be observed that the presence of oscillations is captured correctly, which are primarily the result of the interaction between the controller and the process dynamics. The damping of the oscillations however is slightly underestimated by the model. The transient response of the process to the disturbance is predicted satisfactory for the 1st and 3rd flash vessel, however for the 2nd flash, the model estimates a much larger change, in particular in the pressure, than observed in the measurements.

Noticeable for the 2nd vessel is also the difference in the initial steady-state value of the volumetric flow rate, which is underpredicted by the model by 10 m^3/s, see Fig. 9(d). The difference even increases for off-design. In general, the volumetric vapour flow rate is very sensitive to the temperature and pressure in the vessel. The results indicate that one or both variables are not predicted accu-rately enough by the simulation in order to achieve good agreement in the volumetric flow rate. As no sufficient temperature measure-ments were available for the vessels, possible heat losses along the process have not been included in the model and a comparison of vessel temperatures could not be performed. Concerning the pres-sure, recorded measurements can be subject to biases, hence the actual vessel pressure value might be different than implemented in the model. It is also worth pointing out that saturation is assumed for the vapour flow in the model of the flash vessel. This simplifi-cation leads to an underprediction of the vapour flow rate in case the actual vapour quality is smaller than 1. This might in particular occur during fast pressure transients. These possible reasons for the difference in steady-state values of the volumetric flow would also impact the transient of the pressure control loop of the 2nd vessel. The experimental data and the model prediction for the CO_2 and H_2 content in the 3rd flash vapour flow are depicted in Fig. 9(g) and (h). An offset of 300 s related to sampling and composition analysis has been removed from the experimental data. Overall, very good agreement is observed in terms of transient response but also considering the absolute values, whereby the H_2 content
is marginally underpredicted by the model.

To conclude, with respect to the values of the main process variables at initial steady-state (data recording stopped before all variables reached final steady-state) it can be observed that most of the variables are reproduced with less than 2% error. Larger errors are found, for example, for the volumetric vapour flow rates in the first and second vessels. These deviations are attributed to the uncertainty in predictions for temperatures and/or pressures in the vessels. The dynamic parameters of the transients are predicted with less than 20% error, larger errors are observed for pressure and volumetric vapour flow rate of the second vessel, which are most probably also related to the uncertainties mentioned above. The good agreement between simulation results and experimental data for the CO_2 and H_2 content in the CO_2 product confirms that the composition of the rich solvent flow entering the solvent regeneration section is predicted accurately by the absorber model.

4. Conclusions

The work documented in this paper demonstrates that a well-tuned, equilibrium-based dynamic model for physical absorption of CO_2 provides sufficiently accurate transient performance predictions for the purpose of dynamic process analysis and control system design. The largest deviations between measurements and simulation results were observed during the initial transient of a test whereby a fast change was applied to the lean solvent mass flow rate. This might indicate that either some phenomena which have effect on the response have been neglected or that the model predictions are less accurate for high-frequency response due to fact that the absorber is modelled as the connection of a finite number of volumes at thermodynamic equilibrium. The accuracy of the model predictions during initial transient might be improved by using a rate-based absorber model. A rate-based model however is less suitable for analysis of the entire system comprising the power plant and the capture unit due to the increase in model complexity associated with higher computational effort.

The validated process models have been implemented in an open source library, which serves as reliable basis for the development of models representing a large-scale CO_2 absorption and solvent regeneration unit. The object-oriented modelling approach allows to easily develop new process models by re-use and/or extension of existing models and additional implementation of more sophisticated models if required. The dynamic model of the CO_2 absorption and solvent regeneration unit can be easily combined with a model of the water–gas shift unit to obtain a full model of the pre-combustion CO_2 capture plant. Ultimately, a model of the entire IGCC power plant can be formed by integrating object-oriented models of the gasification unit, the combined cycle and the CO_2 capture plant. Such a system model can be extremely valuable for the design of new plants to support equipment selection and sizing, and to develop and test control strategies. Dynamic simulation is also useful to investigate and ultimately to improve dynamic performance of existing plants.

Acknowledgements

The work documented in this paper has been performed within the CO_2 Catch-up R&D programme aimed at demonstrating and optimizing pre-combustion CO_2 capture technology for the energy sector. This programme is executed in a consortium of Vattenfall, TU Delft and ECN. The authors thankfully acknowledge Kay Damen, Richard Faber and Lukas Valenz, who supervised the execution of the dynamic tests at the pilot plant facility and helped with data collection. The practical advice of the Vattenfall plant operators Perry Brummans, Marc Cuypers and Frans Kornips was invaluable. The authors are grateful to their friend and colleague Teus van der Stelt, who contributed to the model development by improving speed and robustness of the thermophysical property computations.

References

Åkesson, J., Faber, R., Laird, C., Tummescheit, H., Velut, S., Zhu, Y., 2011. Models of a post-combustion absorption unit for simulation, optimization and non-linear model predictive control schemes. In: Proceedings 8th International Modelica Conference, Dresden, Germany.

Aspen Technology, Inc., Aspen Plus V7.3. http://www.aspentech.com, 2013.

Biliyok, C., Lawal, A., Wang, M., Seibert, F., 2012. Dynamic modelling, validation and analysis of post-combustion chemical absorption CO_2 capture plant. Int. J. Greenhouse Gas Control 9, 428–445.

Billet, R., Schultes, M., 1999. Prediction of mass transfer columns with dumped and arranged packings: updated summary of the calculation method of Billet and Schultes. Chem. Eng. Res. Des. 77 (6), 498–504.

Boot-Handford, M., et al., 2014. Carbon capture and storage update. Energy Environ. Sci. 7, 130–189.

Bui, M., Gunawan, I., Verheyen, V., Feron, P., Meuleman, E., Adeloju, S., 2014. Dynamic modelling and optimisation of flexible operation in post-combustion CO_2 capture plants – a review. Comput. Chem. Eng. 61, 245–265.

Cameron, I., Hangos, K., 2001. Process Modelling and Model Analysis. Academic Press.

Casella, F., Colonna, P., 2012. Dynamic modeling of IGCC power plants. Appl. Therm. Eng. 35, 91–111.

Casella, F., Leva, A., 2005. Object-oriented modelling & simulation of power plants with Modelica. In: Proceedings of the 44th IEEE Conference on Decision and Control, and the European Control Conference, CDC-ECC'05, pp. 7597–7602.

Casella, F., Leva, A., 2006. Modelling of thermo-hydraulic power generation processes using Modelica. Math. Comput. Model. Dyn. Syst. 12 (1), 19–33.

Casella, F., Van Putten, J., Colonna, P., 2008. Dynamic simulation of a biomass-fired steam power plant: a comparison between causal and a-causal modular modeling. In: ASME International Mechanical Engineering Congress and Exposition, pp. 205–216.

Chikukwa, A., Enaasen, N., Kvamsdal, H.M., Hillestad, M., 2012. Dynamic modeling of post-combustion CO_2 capture using amines – a review. Energy Procedia 23, 82–91.

Colonna, P., van der Stelt, T., Guardone, A., 2004–2012. FluidProp: A Program for the Estimation of Thermophysical Properties of Fluids. Version 3.0. Software. http://www.FluidProp.com

Damen, K., Troost, M., Faaij, A., Turkenburg, W., 2006. A comparison of electricity and hydrogen production systems with CO_2 capture and storage. Part A: Review and selection of promising conversion and capture technologies. Prog. Energy Combust. Sci. 32, 215–246.

Damen, K., Gnutek, R., Kaptein, J., Nannan, N.R., Oyarzun, B., Trapp, C., Colonna, P., van Dijk, E., Gross, J., Bardow, A., 2011. Developments in the pre-combustion CO_2 capture pilot plant at the Buggenum IGCC. Energy Procedia 4, 1214–1221.

Dietl, K., Joos, A., Schmitz, G., 2012. Dynamic analysis of the absorption/desorption loop of a carbon capture plant using an object-oriented approach. Chem. Eng. Process.: Process Intensif. 52, 132–139.

Dietl, K., 2012. Equation-Based Object-Oriented Modelling of Dynamic Absorption and Rectification Processes (Ph.D. thesis). Hamburg University of Technology.

Fritzson, P., 2003. Principles of Object-Oriented Modeling and Simulation with Modelica 2.1. Wiley.

Gross, J., Sadowski, G., 2001. Perturbed-chain SAFT: an equation of state based on a perturbation theory for chain molecules. Ind. Eng. Chem. Res. 40, 1244–1260.

Harun, N., Nittaya, T., Douglas, P.L., Croiset, E., Ricardez-Sandoval, L.A., 2012. Dynamic simulation of MEA absorption process for CO_2 capture from power plants. Int. J. Greenhouse Gas Control 10, 295–309.

Heil, S., Brunhuber, C., Link, K., Kittel, J., Meyer, B., 2009. Dynamic Modelling of CO_2-removal units for an IGCC power plant. In: Proceedings 7th Modelica Conference, Como, Italy, September 20–22, pp. 77–85.

International Energy Agency (IEA), 2012. CO_2 Emission from Fuel Combustion.

Jayarathna, S., Lie, B., Melaaen, M., 2013. Amine based CO_2 capture plant: dynamic modeling and simulations. Int. J. Greenhouse Gas Control 14, 282–290.

Kale, C., Górak, A., Schoenmakers, H., 2013. Modelling of the reactive absorption of CO_2 using mono-ethanolamine. Int. J. Greenhouse Gas Control 17, 294–308. Koch, I., Hannemann, F., Hoffmann, U., 1999. Dynamic simulation of operating cases and malfunctions of an IGCC power plant fuel system. Chem. Eng. Technol. 22, 568–570.

Kucka, L., Müller, I., Kenig, E., Górak, A., 2003. On the modelling and simulation of sour gas absorption by aqueous amine solutions. Chem. Eng. Sci. 58, 3571–3578.

Kvamsdal, H., Chikukwa, A., Hillestad, M., Zakeri, A., Einbu, A., 2011. A comparison of different parameter correlation models and the validation of an MEA-based absorber model. Energy Procedia 4, 1526–1533.

Lötstedt, P., Petzold, L., 1986. Numerical solution of nonlinear differential equations with algebraic constraints I: Convergence results for backward differentiation formulas. Math. Comput. 46, 491–516.

Lawal, A., Wang, M., Stephenson, P., Yeung, H., 2009. Dynamic modelling of CO_2 absorption for post combustion capture in coal-fired power plants. Fuel 88, 2455–2462.

Lawal, A., Wang, M., Stephenson, P., Koumpouras, G., Yeung, H., 2010. Dynamic modelling and analysis of post-combustion CO_2 chemical absorption process for coal-fired power plants. Fuel 89, 2791–2801.

Mac Dowell, N., Samsatli, N., Shah, N., 2013. Dynamic modelling and analysis of an amine-based post-combustion CO_2 capture absorption column. Int. J. Greenhouse Gas Control 12, 247–258.

Nannan, N.R., de Servi, C.M., van der Stelt, T., Colonna, P., Bardow, A., 2013. An equation of state based on PC-SAFT for physical solvents composed of polyethylene glycol dimethylethers. Ind. Eng. Chem. Res. 52, 18401–18412.

National Energy Technology Laboratory (NETL), 2013. Cost and Performance Baseline for Fossil Energy Plants. Volume 1: Bituminous Coal and Natural Gas to Electricity, September 2013, DOE/NETL-2010/1397, This is revision 2a of the 2010 report.

Posch, S., Haider, M., 2013. Dynamic modeling of CO_2 absorption from coal-fired power plants into an aqueous monoethanolamine solution. Chem. Eng. Res. Des. 91, 977–987.

Prölß, K., Tummescheit, H., Velut, S., Åkesson, J., 2011. Dynamic model of a post-combustion absorption unit for use in a non-linear model predictive control scheme. Energy Procedia 4, 2620–2627.

Taylor, R., Krishna, R., 1993. Multicomponent Mass Transfer. John Wiley and Sons Inc., New York, USA.

Trapp, C., Casella, F., van der Stelt, T.P., Colonna, P., 2014. Use of external fluid property code in Modelica for modelling of a pre-combustion CO_2 capture process involving multi-component two-phase fluids. In: Proceedings 10th Modelica Conference, Lund, Sweden, March 10–12.

Trapp, C., Casella, F., Colonna, P., 2014. Dynamic modelling and validation of a precombustion CO_2 capture plant for control design. Ind. Eng. Chem. Res. 53, 13098–13111.

Trapp, C., 2014. Advances in Model-based Design of Flexible and Prompt Energy Systems – The CO_2 Capture Plant at the Buggenum IGCC Power Station as a Test Case (Ph.D. thesis). Delft University of Technology.

Unger, J., Kröner, A., Marquardt, W., 1995. Structural analysis of differential–algebraic equation systems – theory and applications. Comput. Chem. Eng. 19, 867–882.

Wang, M., Lawal, A., Stephenson, P., Sidders, J., Ramshaw, C., 2011. Post-combustion CO_2 capture with chemical absorption: a state-of-the-art review. Chem. Eng. Res. Des. 89, 1609–1624.

Whittakera, S., Rostron, B., Hawkes, C., Gardner, C., White, D., Johnson, J., Chalaturnyk, R., Seeburger, D., 2011. A decade of CO_2 injection into depleting oil fields: monitoring and research activities of the IEA GHG Weyburn-Midale CO_2 monitoring and storage project. Energy Procedia 4, 6069–6076.

Ziaii, S., Rochelle, G.T., Edgar, T.F., 2011. Optimum design and control of amine scrubbing in response to electricity and CO_2 prices. Energy Procedia 4, 1683–1690.